Tricarboxylic acid cycle activity suppresses acetylation of mitochondrial proteins during early embryonic development in *Caenorhabditis elegans*

Received for publication, July 4, 2018, and in revised form, December 27, 2018 Published, Papers in Press, January 3, 2019, DOI 10.1074/jbc.RA118.004726

Kazumasa Hada[‡§], Keiko Hirota[¶‖], Ai Inanobe[‡‡], Koichiro Kako[¶‖], Mai Miyata[‡‡], Sho Araoi[‡‡], Masaki Matsumoto[§§], Reiya Ohta[¶¶], Mitsuhiro Arisawa[¶¶], Hiroaki Daitoku[‡], Toshikatsu Hanada[§], and Akiyoshi Fukamizu[‡¶‖‖1]**

*From the [‡]Life Science Center for Survival Dynamics, Tsukuba Advanced Research Alliance, University of Tsukuba, 1-1-1 Tennoudai, Tsukuba, Ibaraki 305-8577, Japan, [§]Department of Cell Biology, Faculty of Medicine, Oita University, 1-1 Hasama-machi Idaigaoka, Yufu, Oita, 879-5593, Japan, [¶]Ph.D. Program in Human Biology, School of Integrative and Global Majors, University of Tsukuba, 1-1-1 Tennoudai, Tsukuba, Ibaraki 305-8572, Japan, [‖]Faculty of Life and Environmental Sciences, University of Tsukuba, 1-1-1 Tennoudai, Tsukuba, Ibaraki 305-8572, Japan the, **Department of Hygiene and Public Health, School of Medicine, Tokyo Women's Medical University, 8-1 Kawada-cho, Shinjuku-ku, Tokyo 162-8666, Japan, [‡‡]Graduate School of Life and Environmental Sciences, University of Tsukuba, 1-1-1 Tennoudai, Tsukuba, Ibaraki 305-8572, Japan, [§§]Medical Institute of Bioregulation, Kyushu University, 3-1-1 Maidashi, Fukuoka, Fukuoka 812-8582, Japan, [¶¶]Graduate School of Pharmaceutical Sciences, Osaka University, 1-6 Yamada-oka, Suita, Osaka 565-0871, Japan, and [‖‖]International Institute for Integrative Sleep Medicine (WPI-IIIS), University of Tsukuba, 1-1-1 Tennoudai, Tsukuba, Ibaraki 305-8575, Japan*

Edited by John M. Denu

The tricarboxylic acid (TCA) cycle (or citric acid cycle) is responsible for the complete oxidation of acetyl-CoA and formation of intermediates required for ATP production and other anabolic pathways, such as amino acid synthesis. Here, we uncovered an additional mechanism that may help explain the essential role of the TCA cycle in the early embryogenesis of *Caenorhabditis elegans*. We found that knockdown of citrate synthase (*cts-1*), the initial and rate-limiting enzyme of the TCA cycle, results in early embryonic arrest, but that this phenotype is not because of ATP and amino acid depletions. As a possible alternative mechanism explaining this developmental deficiency, we observed that *cts-1* RNAi embryos had elevated levels of intracellular acetyl-CoA, the starting metabolite of the TCA cycle. Of note, we further discovered that these embryos exhibit hyperacetylation of mitochondrial proteins. We found that supplementation with acetylase-inhibiting polyamines, including spermidine and putrescine, counteracted the protein hyperacetylation and developmental arrest in the *cts-1* RNAi embryos. Contrary to the hypothesis that spermidine acts as an acetyl sink for elevated acetyl-CoA, the levels of three forms of acetylspermidine, N^1-acetylspermidine, N^8-acetylspermidine, and N^1,N^8-diacetylspermidine, were not significantly increased in embryos treated with exogenous spermidine. Instead, we demonstrated that the mitochondrial deacetylase sirtuin 4 (encoded by the *sir-2.2* gene) is required for spermidine's suppression of protein hyperacetylation and developmental arrest in the *cts-1* RNAi embryos. Taken together, these results suggest the possibility that during early embryogenesis, acetyl-CoA consumption by the TCA cycle in *C. elegans* prevents protein hyperacetylation and thereby protects mitochondrial function.

The tricarboxylic acid (TCA)[2] cycle plays pivotal roles in not only the production of metabolic intermediates, but also the developmental processes in metazoan. Several studies have elucidated that the TCA cycle inhibitor fluoroacetate blocks the development of 1-cell or 2-cell embryos in rabbits and mice (1, 2). Moreover, down-regulation of genes for the TCA cycle components has been shown to hamper early embryogenesis in *Caenorhabditis elegans* (3, 4). Thus, although the TCA cycle is essential for early embryonic development, its molecular mechanism remains poorly understood.

The starting point for the TCA cycle is acetyl-CoA that reacts with oxaloacetate to form citrate, which is then oxidized to CO_2 for ATP production in the cycle. In addition, acetyl-CoA is used for the acetylation reaction as a donor of the acetyl group that is transferred to α-amino groups of N-terminal amino acids or the ϵ-amino group of lysine residues of proteins as well as amino groups of metabolites, such as polyamines (5).

Reversible protein acetylation is a major regulatory mechanism for controlling protein function. In the nucleus, reversible acetylation of histones and transcription factors through acetyltransferases and deacetylases plays central roles in the regulation of gene expression (6). Likewise, mitochondria have been shown to harbor numerous acetylated proteins; namely 63% of mitochondrial proteins contain lysine acetylation sites (7). However, unlike the nucleus, mitochondrial acetylation is

This work was supported by Grant-in-Aid Project 23116001 (Scientific Research on Innovative Areas) from the Ministry of Education, Culture, Sports, Science and Technology (MEXT) (to A. F.) and the Japan and Grants-in-Aid for Scientific Research (A) 17H01519 (to A. F.); Grants-in-Aid for Scientific Research (C) 26450119 and 17K07746 (to K. H.), 26350957 and 17K01942 (to K. K.), and 17K08193 (to H. D.) from the Japan Society for the Promotion of Science. The authors declare that they have no conflicts of interest with the contents of this article.

This article contains supporting experimental procedures, Figs. S1–S3, and Tables S1 and S2.

[1] To whom correspondence should be addressed. Tel.: 81-29-853-6070; Fax: 81-29-853-6070; E-mail: akif@tara.tsukuba.ac.jp.

[2] The abbreviations used are: TCA, tricarboxylic acid; CE, capillary electrophoresis; IB, isolation buffer; TL, total lysate; MP, mitochondrial pellet; PMS, post-mitochondrial supernatant; Spd, spermidine.

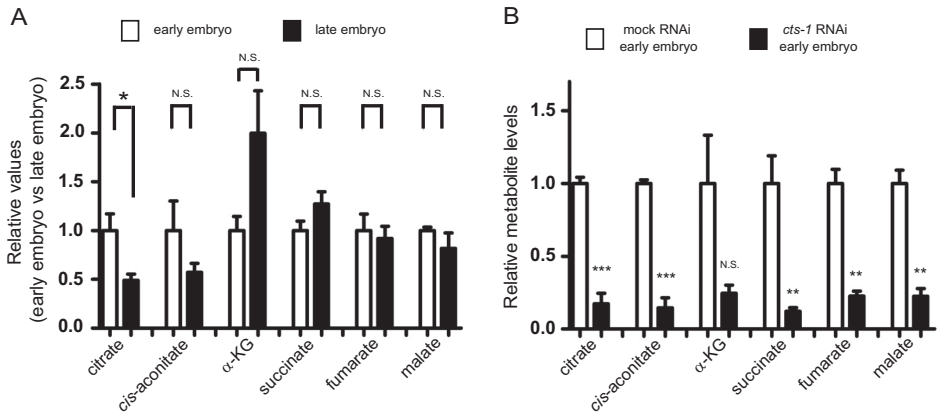

Figure 1. Citrate is decreased from the early to late embryonic stage in *C. elegans*. *A*, the relative values of the TCA cycle metabolites between the early and late embryonic stages. The levels of each TCA cycle metabolite were normalized to the amounts of total TCA cycle metabolites at each developmental stage and indicated as relative value (early embryo *versus* late embryo). Data are mean ± S.E.; $n > 5$; *, $p < 0.05$; *N.S.*, not significant. α-KG indicates α-ketoglutarate. *B*, the levels of the TCA metabolites in mock and *cts-1* RNAi embryos with CE-TOF/MS. Data are mean ± S.E.; $n = 3$; **, $p < 0.01$; ***, $p < 0.001$; *N.S.*, not significant.

thought to be largely elicited by nonenzymatic reaction of reactive lysine residues with acetyl-CoA and removed by the mitochondrial NAD^+-dependent deacylase SIRT3 (8–11). It should be noted that protein acetylation in mitochondria typically results in dysfunction of various major aspects of mitochondrial biology.

It was previously reported that acetyl-CoA levels were elevated and proteins were acetylated in mitochondria when fuel was increased (12). Furthermore, current evidence suggests that acetyl-CoA is a key factor determining the levels of protein acetylation during early embryonic development in *Xenopus laevis* (13). Given that elevated acetyl-CoA levels could induce protein lysine acetylation in mitochondria, we hypothesized that the consumption of acetyl-CoA through the TCA cycle is an indispensable process for maintaining normal mitochondrial function. Here we provide a functional relationship between the TCA cycle and mitochondrial protein hyperacetylation during early embryonic development in *C. elegans*.

Results

Citrate is consumed predominantly from the early to late embryonic stage in C. elegans

To understand the role of the TCA cycle during embryogenesis, we first measured the levels of metabolites of the TCA cycle at both the early and late embryonic stages in *C. elegans*. LC-MS analysis showed that the relative ratio of citrate, but not other metabolites of the TCA cycle, is significantly decreased in the late embryos (Fig. 1*A*). Given that citrate is consumed and then regenerated by the sequence of reactions to complete the TCA cycle, the reduction of citrate at the late embryonic stage implies a contribution of the TCA cycle to the process of embryogenesis. To investigate whether the consumption of citrate is an essential process involved in embryogenesis, we focused on citrate synthase encoded by *cts-1* gene that is the initial and rate-limiting enzyme of the TCA cycle. As shown in Fig. 1*B*, the levels of all TCA metabolites in early embryos were markedly decreased when *cts-1* was silenced by feeding RNAi. Thus, *cts-1* knockdown approach has allowed us to clarify the role of citrate consumption in early embryogenesis.

cts-1 knockdown causes developmental arrest at the early embryonic stage without lack of intracellular ATP levels

The TCA cycle is an oxidative device coupled to the electron transport chain for the production of ATP and the genes responsible for the electron transport chain are known to be required for early embryogenesis (4). Because *cts-1* knockdown led to dysfunction of the TCA cycle, we hypothesized that *cts-1* RNAi animals exhibit early developmental defects. As expected, *cts-1* knockdown dramatically reduced hatching rate and also caused developmental arrest at the early embryonic stage (Fig. 2, *A* and *B*). Next, to test whether these phenotypes result from a failure of ATP production by *cts-1* knockdown, we measured ATP levels in mock or *cts-1* RNAi embryos using CE-TOF/MS. Surprisingly, however, the ATP levels of *cts-1* RNAi embryos were comparable with those of mock RNAi embryos (Fig. 2*C*). Similar result was obtained using the luciferase-luciferin system (Fig. S1*A*). These data suggest that energy shortage is not a cause of early embryonic arrest in *cts-1* RNAi animals.

A reduction in the levels of glutamate, aspartate, and citrate is not a cause of early embryonic arrest by cts-1 knockdown

Several amino acids are synthesized from TCA metabolites, including α-ketoglutarate and oxaloacetate. Thus, homeostatic imbalance of amino acids could be a possible explanation for early embryonic arrest by *cts-1* knockdown. To test this hypothesis, we quantified the relative amounts of amino acids using CE-TOF/MS and found that glutamate and aspartate, which are derived from α-ketoglutarate and oxaloacetate, respectively, were decreased in *cts-1* RNAi embryos as compared with mock control (Fig. S1, *B* and *C*). Next, to determine whether reduction of glutamate and aspartate is sufficient to account for early embryonic arrest by *cts-1* knockdown, we supplemented *cts-1* RNAi embryos with an excess dose (30 mM) of glutamate and aspartate and examined hatching rate. Although the levels of glutamate and aspartate in *cts-1* RNAi embryos were completely restored by the supplementation, this treatment failed to rescue the reduced hatching rate even when both glutamate and aspartate were added (Fig. 2, *D–F*). These observations

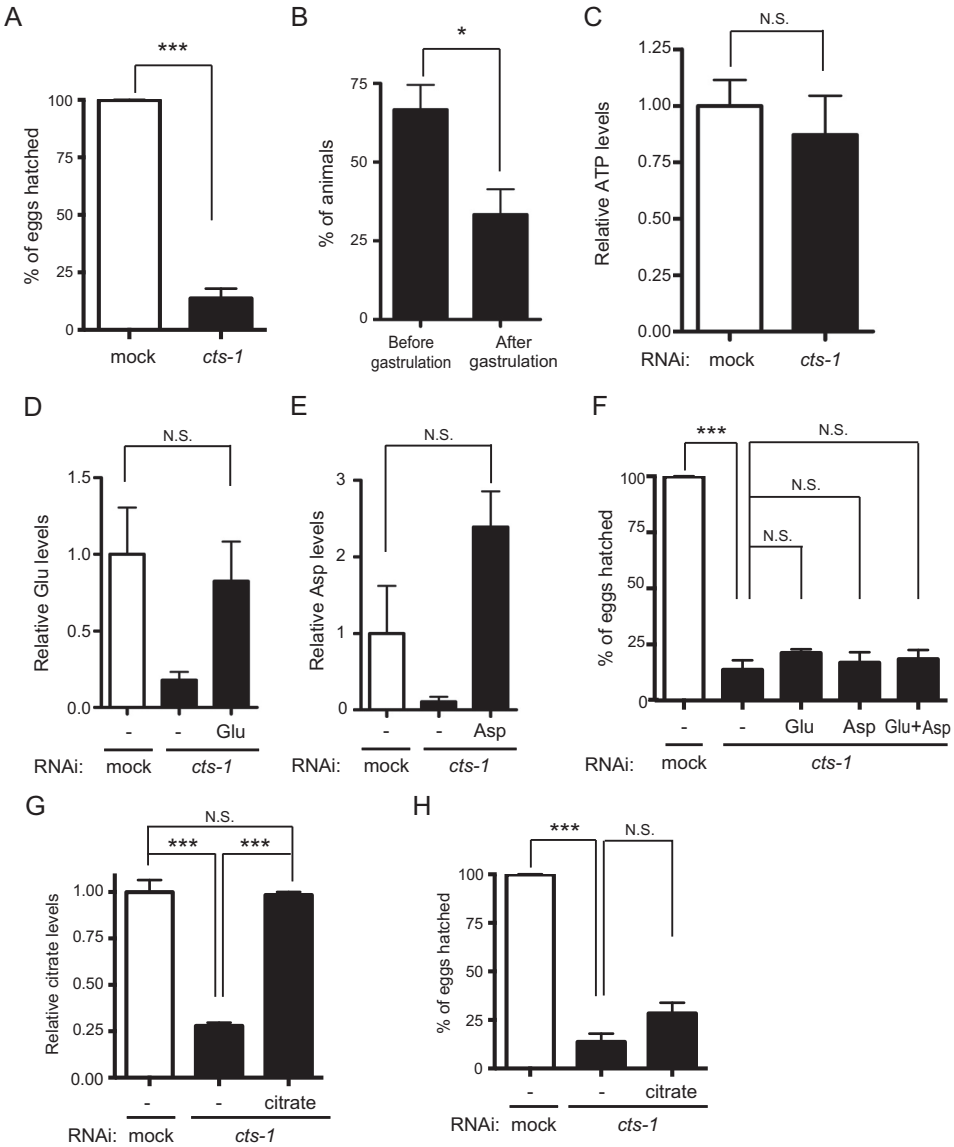

Figure 2. *cts-1* knockdown results in early embryonic arrest without depletion of intracellular ATP levels. *A*, the hatching rate in mock and *cts-1* RNAi embryos (data are mean ± S.E.; $n = 3$; ***, $p < 0.001$). *B*, percentage of animals at each embryonic stage in *cts-1* RNAi embryos (data are mean ± S.E.; *, $p < 0.05$). *C*, ATP levels in mock and *cts-1* RNAi embryos with CE-TOF/MS (*N.S.*, not significant). *D*, the levels of glutamate in mock RNAi embryos with vehicle (−), *cts-1* RNAi embryos with vehicle (−), and 30 mM glutamate (*Glu*) with LC-MS/MS (data are mean ± S.E.; $n = 3$; *N.S.*, not significant). *E*, the levels of aspartate in mock RNAi embryos with vehicle (−), *cts-1* RNAi embryos with vehicle (−), and 30 mM aspartate (*Asp*) with LC-MS/MS (data are mean ± S.E.; $n = 3$; *N.S.*, not significant). *F*, the hatching rate of mock RNAi embryos with vehicle (−), *cts-1* RNAi embryos with vehicle (−), and 30 mM Glu and/or Asp (data are mean ± S.E.; $n = 3$; ***, $p < 0.001$, *N.S.*, not significant). *G* and *H*, citrate levels (*G*) and the hatching rate (*H*) in mock RNAi embryos with vehicle (−) and *cts-1* RNAi embryos with vehicle (−), and 30 mM citrate (data are mean ± S.E.; $n = 3$; ***, $p < 0.001$; *N.S.*, not significant).

imply that decreased levels of glutamate and aspartate do not account for early embryonic arrest by *cts-1* knockdown.

Alternatively, because it has been reported that citrate allosterically modulates metabolic enzymes, such as phosphofructokinase, pyruvate kinase, pyruvate dehydrogenase, and acetyl-CoA carboxylase, thereby controlling glycolysis and fatty acid synthesis (14), we assessed a direct effect of citrate depletion on the embryogenesis by adding back citrate to *cts-1* RNAi embryos. However, consistent with the results of amino acid supplementation (Fig. 2, *D–F*), addition of citrate had no effect on the reduced hatching rate in *cts-1* RNAi embryos, despite the fact that citrate levels were recovered to those in mock RNAi embryos (Fig. 2, *G* and *H*). Taken together, these results suggest that early embryonic arrest by *cts-1* knockdown is not attributed to reduced levels of glutamate, aspartate, and citrate in *C. elegans*.

cts-1 RNAi embryos show an increase in the levels of acetyl-CoA and acetylation of mitochondrial proteins

As referred to above, our results demonstrated that at least production of ATP, amino acids, and citrate through the TCA cycle does not play a critical role in the hatching process of *C. elegans.* If so, what is the role of the TCA cycle in early embryogenesis? To find a clue to address this question, we performed LC-MS/MS analysis with mock and *cts-1* RNAi embryos and found that acetyl-CoA, the starting point for the TCA cycle, is significantly increased by *cts-1* knockdown (Fig. 3*A*). This finding raised the possible involvement of acetyl-CoA

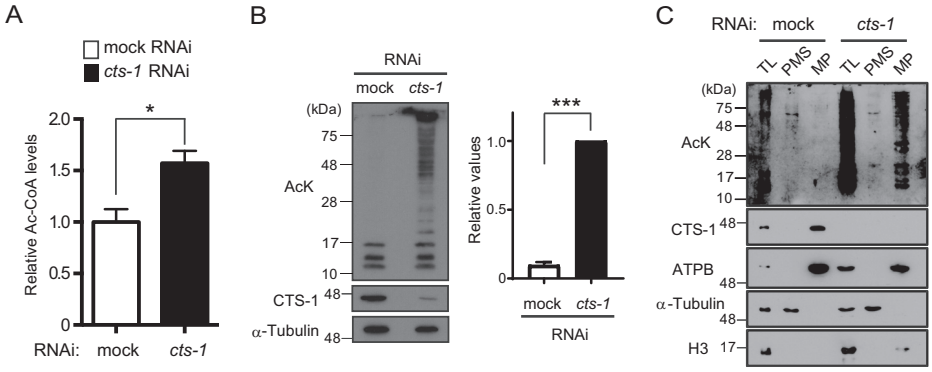

Figure 3. *cts-1* knockdown causes an increase in acetyl-CoA levels and mitochondrial protein hyperacetylation in early embryos. *A*, the levels of acetyl-CoA in mock and *cts-1* RNAi embryos with LC-MS/MS. Data are mean ± S.E.; $n = 3$; *, $p < 0.05$. *B*, *left*, acetylated proteins of mock RNAi embryos and *cts-1* RNAi embryos (*AcK*, acetylated proteins; *CTS-1*, citrate synthase-1). *Right*, the levels of total acetylated proteins larger than 28 kDa in mock and *cts-1* RNAi embryos (data are mean ± S.E.; $n = 3$; ***, $p < 0.001$). *C*, acetylated proteins of total lysate (TL), post-mitochondrial supernatant (PMS), or mitochondrial pellets (MP) in mock and *cts-1* RNAi embryos (*ATPB*, ATP synthase β; *H3*, histone H3).

in early embryogenesis, and because acetyl-CoA serves as an acetyl donor for the acetylation as well as a source of ATP, we tested whether elevated levels of intracellular acetyl-CoA promotes acetylation of proteins in *cts-1* RNAi embryos. Expectedly, Western blotting with an anti-acetyl lysine antibody showed that although only a few bands, probably histones, are detected as acetylated proteins in mock control, *cts-1* knockdown apparently enhances the acetylation of a wide range of proteins (Fig. 3*B*). Next, to determine in which cellular compartment(s) hyperacetylation occurs in *cts-1* RNAi embryos, we focused on mitochondria where the elevation of acetyl-CoA levels has been shown to induce lysine acetylation (12). Total lysates from mock and *cts-1* RNAi embryos were separated into mitochondrial and post-mitochondrial fractions as verified by Western blotting with organelle markers, and an increased acetylation was observed exclusively in mitochondrial fraction of *cts-1* RNAi embryos (Fig. 3*C*). These data were further confirmed by proteome analysis, showing that a number of mitochondrial proteins, such as ACO-2, ATP-3, and HSP-6, are acetylated to a greater extent by *cts-1* knockdown (Fig. S2).

Polyamine application counteracts protein hyperacetylation and developmental arrest in cts-1 RNAi embryos

Next, we attempted to investigate whether early embryonic arrest by *cts-1* knockdown would be because of aberrant hyperacetylation of proteins in *C. elegans*. To this end, as a potent acetylase inhibitor, we adopted the naturally occurring polyamines: spermidine and putrescine. It has been reported that spermidine inhibits acetyltransferase activity and its decline with age leads to hyperacetylation, early necrotic death, and decreased life span (15, 16). Besides, putrescine is interconvertible with spermidine. Exogenous supply of putrescine and spermidine to *cts-1* RNAi animals caused a marked decrease in the extent of protein acetylation (Fig. 4*A*). Importantly, we found that the same experimental conditions enable amelioration of a reduced hatching rate of *cts-1* RNAi embryos (Fig. 4*B*). On the other hand, polyamine treatment had no recovery effect on decreases in TCA metabolites and amino acids, glutamate and aspartate (Figs. S3, *A–C*). Taken together, these results suggest that the proper progression of the TCA cycle could be required for normal embryogenesis to prevent aberrant hyperacetylation of mitochondrial proteins in *C. elegans*.

Spermidine does not act as a sink for the elevated acetyl-CoA levels even when treated with high dose

Although the rescue effect of polyamine in embryogenesis would be achieved through inhibition of hyperacetylation because of overproduction of acetyl-CoA, the detailed mechanism how polyamine reduces protein acetylation remains unclear. Meanwhile, we noticed key findings from the CE-TOF/MS data demonstrating that *cts-1* knockdown augments the levels of acetylated polyamines, namely, acetylputrescine and acetylspermidine (Fig. 5*A*). These emerging data prompted us to consider that excess concentrations of polyamines might be sinks for the elevated acetyl-CoA levels as acetylation acceptors, thereby siphoning off the amount of acetyl-CoA for protein acetylation. To test this hypothesis, we set up to determine the levels of acetylspermidine in mock and *cts-1* RNAi embryos treated with or without spermidine. Because amino groups of spermidine are acceptable for acetylation at both its ends (Fig. 5*B*), the two distinct mono- (N^1- and N^8-acetylspermidine) and the diacetylated (N^1,N^8-diacetylspermidine) forms of spermidine were measured specifically using LC-MS/MS. Unexpectedly, however, we found that the levels of all forms of acetylspermidine in *cts-1* RNAi embryos are not significantly increased when treated with exogenous spermidine (Fig. 5, *C–E*). A similar result was observed in the levels of acetylputrescine (data not shown). These data indicate that polyamine-mediated inhibition of protein hyperacetylation is not attributed to the function of spermidine as a sink for acetyl groups under overproduction of acetyl-CoA.

sir-2.2 is required for recovery effect of spermidine on protein hyperacetylation and developmental arrest in cts-1 RNAi embryos

An alternative possible mechanism for polyamine-mediated inhibition of hyperacetylation could be the activation of protein deacetylase. Considering that polyamine treatment inhibited protein hyperacetylation occurring primarily in mitochondria, potential targets of polyamine should be the mitochondrial deacetylases, including three sirtuin isoforms, SIRT3, SIRT4, and SIRT5. Among them, mammalian SIRT3 is the major protein deacetylase in mitochondria (10), but there are no genes with similarity to SIRT3 and also SIRT5 in *C. elegans*. Instead,

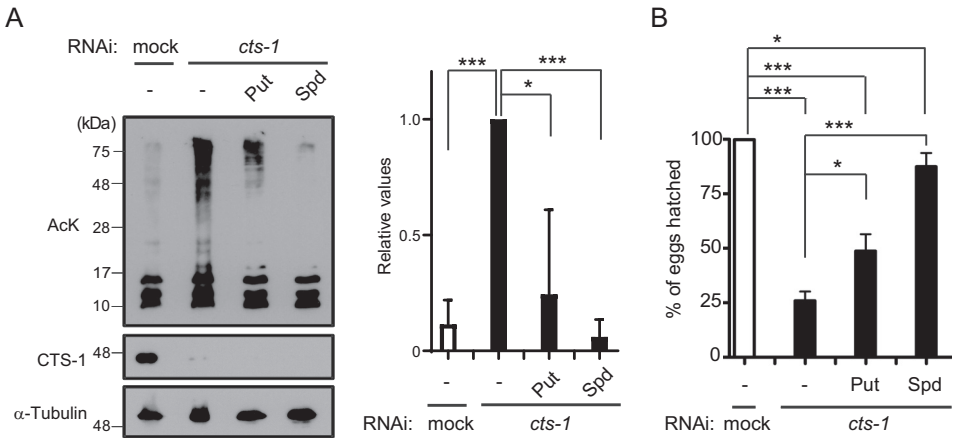

Figure 4. Polyamine supplementation counteracts protein hyperacetylation and decreased hatching rates in *cts-1* RNAi embryos. A, *left*, acetylated proteins in mock RNAi embryos with vehicle (−) and *cts-1* RNAi embryos with vehicle (−), putrescine (*Put*), or spermidine (*Spd*). *Right*, the levels of total acetylated proteins larger than 28 kDa in mock and *cts-1* RNAi embryos supplemented with or without Put or Spd (data are mean ± S.E.; $n = 3$; ***, $p < 0.001$; *, $p < 0.05$). *B*, the hatching rate of mock RNAi embryos with vehicle (−) and *cts-1* RNAi embryos with vehicle (−), Put, or Spd (data are mean ± S.E.; $n = 3$; *, $p < 0.05$; ***, $p < 0.001$).

C. elegans possesses two genes, *sir-2.2* and *sir-2.3*, both of which are orthologs of SIRT4 and their products are localized in mitochondria (17). However, because *C. elegans* SIR-2.2 and SIR-2.3 proteins have not been demonstrated to catalyze deacetylation on a variety of substrates, we first examined broad deacetylase activity of SIR-2.2 in mock and *cts-1* RNAi embryos. As shown in Fig. 6*A*, we found that although endogenous protein acetylation levels of early embryos are comparable between WT N2 and *sir-2.2(tm2648)* mutant animals, *cts-1* knockdown-induced hyperacetylation of proteins larger than 28 kDa is slightly augmented in *sir-2.2(tm2648)* mutant, suggesting that SIR-2.2 contributes to protein deacetylation, at least, when acetyl-CoA levels are elevated.

We next investigated the role of *sir-2.2* in spermidine-mediated inhibition of protein hyperacetylation under *cts-1* knockdown condition. Notably, the inhibitory effect of spermidine on protein hyperacetylation in *cts-1* RNAi embryos was completely abolished by deletion of *sir-2.2* gene (Fig. 6*B*). In contrast, spermidine treatment substantially decreased the *cts-1* knockdown-induced hyperacetylation in *sir-2.3(ok444)* mutants (Fig. 6*C*), indicating that not *sir-2.3*, but *sir-2.2* is involved in the spermidine-mediated inhibition of protein hyperacetylation. Finally, we examined hatching rate of WT N2 and deletion mutants of *sir-2.1* (the SIRT1 ortholog), *sir-2.2*, and *sir-2.3* to ascertain whether *sir-2.2* indeed plays a role in the spermidine-mediated recovery of embryonic development. As expected, the reduced hatching rates by *cts-1* knockdown were observed in all strains tested, whereas the recovery effect of spermidine was partially abrogated in the *sir-2.2(tm2468)* mutant compared with N2 and other mutants (Fig. 6*D*). Taken together, these results imply that SIR-2.2 is a target of spermidine for preventing hyperacetylation when the TCA cycle is impaired during early embryogenesis.

Discussion

The fundamental question in this study is what the role of the TCA cycle during embryogenesis in *C. elegans* is. We demonstrated that the TCA cycle is indispensable for early embryonic development by RNAi depletion of CTS-1 that functions as the initial and rate-limiting enzyme of the TCA cycle (Fig. 1, *A* and *B*). Although ATP deprivation appeared to be a cause of early developmental arrest in *cts-1* RNAi embryos, there was no difference in intracellular ATP levels between control and *cts-1* RNAi embryos (Figs. 1*C* and S1*A*). This finding indicates that intracellular ATP levels are sustained during early embryogenesis even without ATP production through the TCA cycle. If so, what pathways are used for supplying ATP? We consider two possibilities: (1) through glycolysis and (2) through amino acid metabolism. To address this issue, we treated early embryos with 2-deoxyglucose, a glycolysis inhibitor, but no decrease was observed in ATP levels (data not shown), suggesting that glycolysis is not likely to participate in ATP supply during early embryogenesis. Another possibility is the use of amino acid as a substitute for acetyl-CoA to produce ATP. An interesting model has been proposed in which the TCA cycle reactions are split into complementary mini-cycles: namely, the first mini-cycle converts α-ketoglutarate to oxaloacetate and the second mini-cycle converts oxaloacetate to α-ketoglutarate (18). Based on this model, the first mini-cycle would allow metabolizing glutamate for producing ATP even when the second mini-cycle does not function by *cts-1* knockdown. Supporting this notion, we found that the levels of glutamate are considerably decreased in *cts-1* RNAi embryos (Fig. S1*B*). Instead, the existence of multiple metabolic pathways to ensure the level of intracellular ATP implies other roles of the TCA cycle in early embryonic development.

Here, we demonstrated the relationship between the TCA cycle and protein/metabolite acetylation through acetyl-CoA. The primary function of the TCA cycle is to release stored energy through the oxidation of acetyl-CoA into carbon dioxide and chemical energy in the form of ATP. As mentioned above, however, we revealed that ATP levels are not influenced by *cts-1* knockdown and rather successive consumption of acetyl-CoA via the TCA cycle plays a crucial role in preventing accumulation of acetyl-CoA in mitochondria (Fig. 3*A*). Given that mitochondrial proteins possessing intrinsic acetyltransferase activity have not been identified so far (9), excessive accumulation of acetyl-CoA exclusively in mitochondria seems to cause aberrant acetylation of proteins and metabolite through

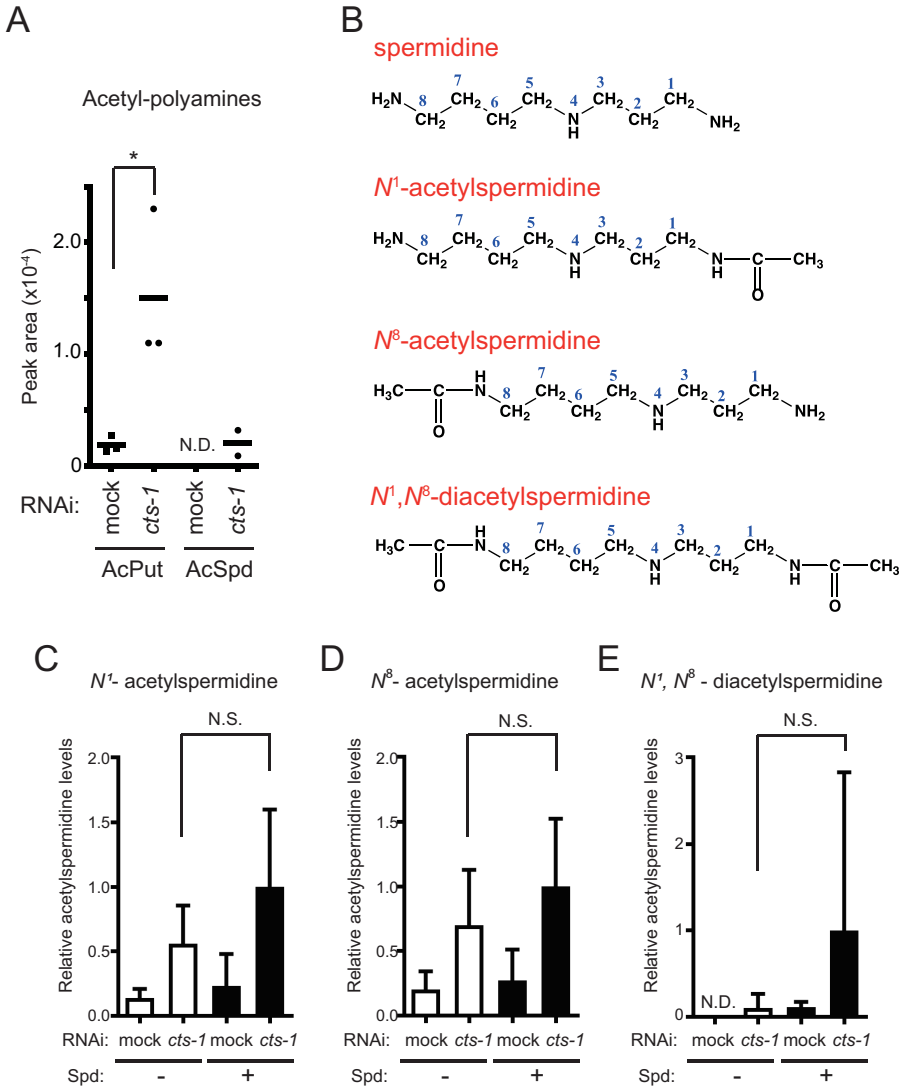

Figure 5. Spermidine does not act as an acetyl sink even when treated with high-dose. *A*, relative areas of acetyl polyamines in mock and *cts-1* RNAi embryos with CE-TOF/MS (data are mean ± S.E.; $n = 3$; *, $p < 0.05$). *B*, structural formula of acetylated spermidines, N^1-acetylspermidine (*top*), N^8-acetylspermidine (*middle*), and N^1,N^8-diacetylspermidine (*bottom*). *C–E*, the levels of acetylated spermidines, (*C*) N^1-acetylspermidine, (*D*) N^8-acetylspermidine, and (*E*) N^1,N^8-diacetylspermidine, in mock RNAi embryos with vehicle (−), *cts-1* RNAi embryos with vehicle (−), mock RNAi embryos with Spd (+), and *cts-1* RNAi embryos with Spd (+) with LC-MS/MS. The *y* axis values indicate each acetylspermidine level relative to that of *cts-1* RNAi embryos treated with Spd (data are mean ± S.E.; $n = 4$; *N.D.*, not detected; *N.S.*, not significant).

the nonenzymatic reaction, thereby resulting in mitochondrial dysfunction related to early embryonic arrest. Moreover, it is noted that a large number of mitochondrial proteins involved in metabolic pathways have been shown to be regulated by reversible acetylation (7). Taken together, we suggest the notion that homeostatic modulation of mitochondrial protein acetylation could be an alternative function of the TCA cycle at least during embryogenesis. Meanwhile, because blocking citrate synthase would have a number of effects beyond producing an excess amount of acetyl-CoA, it is important to provide evidence that increasing acetylation of mitochondrial proteins by a method except *cts-1* knockdown also leads to mitochondrial dysfunction and early embryonic lethality.

To prevent hyperacetylation of mitochondrial proteins, we used natural polyamines, such as spermidine, which has been reported to inhibit histone acetyltransferases and thereby promote longevity through up-regulation of autophagy-related transcripts (15). In addition to the fact that a definitive mitochondrial acetyltransferase has not been identified, our findings from metabolome analysis led to the hypothesis that excess concentrations of polyamines might be sinks for the elevated acetyl-CoA levels by being acetylated themselves and thus siphon off the amount of acetyl-CoA for protein acetylation. However, because no significant increase in the levels of acetyl forms of spermidine, including N^1-acetylspermidine, N^8-acetylspermidine, and N^1,N^8-diacetylspermidine, was observed even when the TCA cycle was compromised by *cts-1* knockdown (Fig. 5), this hypothesis appears to be incorrect at least in our experimental conditions. Instead, we discovered that the nematode mitochondrial sirtuin, SIR-2.2, has deacetylase activity, albeit at a lower level, and could be a target of spermidine-mediated inhibition of hyperacetylation (Fig. 6). Although we are unable to uncover the molecular mechanism underlying the action of polyamine on SIR-2.2 function, our findings provide

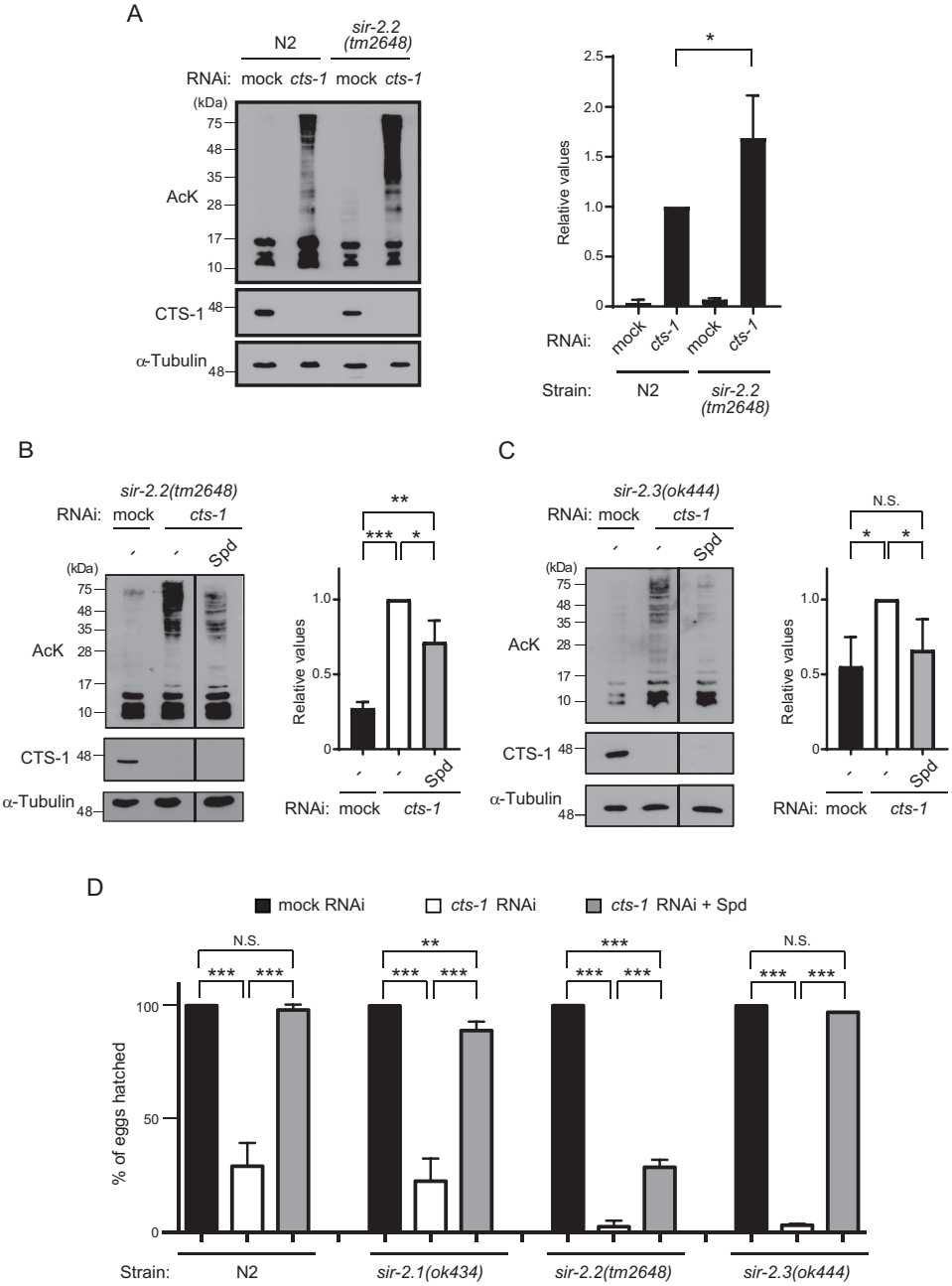

Figure 6. *sir-2.2* is necessary for recovery effect of spermidine on protein hyperacetylation and developmental arrest in *cts-1* RNAi embryos. *A*, *left*, Western blotting of acetylated proteins of mock RNAi embryos and *cts-1* RNAi embryos in WT and *sir-2.2*(*tm2648*). *Right*, the levels of total acetylated proteins larger than 28 kDa in mock and *cts-1* RNAi embryos of N2 or *sir-2.2*(*tm2648*) (data are mean ± S.E.; $n = 3$; *, $p < 0.05$; *N.S.*, not significant). *B* and *C*, *left*, acetylated proteins of mock RNAi embryos with vehicle (−) and *cts-1* RNAi embryos with vehicle (−) or Spd in *sir-2.2*(*tm2648*) (*B*) and *sir-2.3*(*ok444*) (*C*) mutants. *Right*, the levels of total acetylated proteins larger than 28 kDa in mock and *cts-1* RNAi embryos of *sir-2.2*(*tm2648*) (*B*) and *sir-2.3*(*ok444*) treated with or without Spd (data are mean ± S.E.; $n = 3$; ***, $p < 0.001$; **, $p < 0.01$; *, $p < 0.05$; *N.S.*, not significant). *D*, the hatching rate of mock RNAi embryos with vehicle (−) and *cts-1* RNAi embryos with vehicle (−) or Spd in N2, *sir-2.1*(*ok434*), *sir-2.2*(*tm2648*), and *sir-2.3*(*ok444*) mutants (data are mean ± S.E.; $n = 3$; **, $p < 0.01$; ***, $p < 0.001$; *N.S.*, not significant).

new insight into the physiological significance of polyamine as an acetylation inhibitor.

Interestingly, it was reported that N^1,N^8-diacetylspermidine is a potential cancer marker for early detection because its levels in the urine from patients are increased along with a progression of cancer (20). However, to date, there is no report describing the existence of N^1,N^8-diacetylspermidine in animals other than human and it remains unknown how N^1,N^8-diacetylspermidine is produced in cancer cells. In this study, we first discovered the endogenous production of N^1,N^8-diacetylspermidine in nematode when the TCA cycle is compromised by *cts-1* knockdown (Fig. 5*E*). Considering that N^1,N^8-diacetylspermidine is predicted to arise simultaneously with the accumulation of mitochondrial acetyl-CoA, this diacetylpolyamine could be a biomarker that identifies the metabolic balance between glycolysis and the TCA cycle.

Our present study revealed a possible link among the TCA cycle, acetylation, and polyamine at the stage of early embryonic development in *C. elegans*. On the other hand, it is likely that this mutual relationship plays an important role in various

biological phenomena throughout life. In particular, considering that spermidine is a longevity drug that can increase life span in yeast, nematodes, and flies (15), the acetylation status mediated by the TCA cycle is emerging as a promising regulatory mode of chronological aging. Consistent with this notion, a glucose-enriched diet has been shown to shorten life span by down-regulating the DAF-16 and HSF-1 transcription factors in *C. elegans* (21). Further investigations of the relationship between the TCA cycle and protein/metabolite acetylation in view of metabolic change with age will shed light on how spermidine increases longevity and also contributes to identify therapies to slow down aging and delay age-associated diseases.

Experimental procedures

Strains and the maintenance

Bristol N2 WT, *sir-2.1(ok434)*, and *sir-2.3(ok444)* were provided by the Caenorhabditis Genetics Center (CGC). *sir-2.2(tm2468)* was obtained from National BioResource Project (NBRP). All mutants were backcrossed five times to N2. All strains were maintained on Nematode Growth Medium plates at 20 °C.

Collection of animals

To suppress the loss of the collected embryos and metabolites through the nonspecific adsorption with tubes and tips, we used platinum tubes and tips (BM-Bio Inc.) in all experiments.

Reagents and antibodies

Reagents were purchased from Sigma-Aldrich, Wako, Tokyo-INC, Tokyo Chemical Industry, Cambridge Isotope Laboratories, Inc., and Cayman Chemical Co. Antibodies were purchased from Santa Cruz Biotechnology, Cell Signaling Technology, MBL International, and Abcam. N^1,N^8-diacetylspermidine was chemically synthesized and purified. The detailed information on reagents and antibodies is shown in Table S1.

Sample preparation for metabolite measurement

Early and late embryos were collected immediately and 11–12 h after bleaching of 5000 gravid adults, respectively. Embryos of mock RNAi or *cts-1* RNAi were collected after thorough bleaching of ~14,000 or 27,000 gravid adults, respectively. The embryonic pellets were stored at −80 °C.

LC-MS or LC-MS/MS analysis

Chilled methanol and internal standards were added to the embryonic pellet. The mixture was sonicated. Metabolites were extracted by addition of chloroform and water. The upper phase was carefully transferred into new tubes and dried with a rotary concentrator at 4 °C. The dried pellet was resuspended in MS-grade distilled water and centrifuged. The supernatant was utilized for LC-MS and LC-MS/MS. Detailed procedures for LC-MS or LC-MS/MS analysis are shown in supporting experimental procedures (Table S2).

RNAi experiments and metabolite supplementation

Synchronized L1 animals were grown on Nematode Growth Medium plates seeded with *Escherichia coli* (OP50). Two hundred early L4 animals were transferred to RNAi plates containing ampicillin (100 mg/L) and isopropyl 1-thio-β-D-galactopyranoside (1.0 mM) seeded with *E. coli* (HT115) expressing target gene dsRNA, and embryos were examined after 45 h of RNAi treatment. In supplementation with metabolites, we prepared RNAi plates seeded with *E. coli* (HT115) and dropped metabolite water solution onto the surface of the agar so that final concentration was 30 mM or 60 mM, and then dried it just before transferring early L4 animals to RNAi plates. In this study, we used the plates as 30 mM or 60 mM metabolite supplementation plates.

Metabolome analysis with CE-TOF/MS

Chilled methanol and internal standards were added to the embryonic pellet. The mixture was sonicated four times. For metabolome analysis, the mixture was deproteinized with 5 kDa MW cutoff spin filter. The filtrate was frozen in liquid nitrogen and stored at −80 °C until use. The large-scale measurements and data processing of metabolites were performed through a facility service at Human Metabolome Technologies, Inc. (Tsuruoka, Japan).

Western blot analysis

Early L4 animals were bred on RNAi plates for 45 h. Embryos of mock RNAi or *cts-1* RNAi were collected after thorough bleaching ~3000 or 4000 gravid adults, respectively. The embryonic pellets were boiled in 50 μl of 1× SDS-PAGE sample buffer (50 mM Tris-HCl, pH 7.5, 1.8% mercaptoethanol, 1% SDS, 0.01% bromphenol blue, 10% glycerol). Then, 5–10 μl of the lysates were separated on 15% SDS-PAGE, and then the proteins were transferred to PVDF membrane. The membrane was treated with the blocking buffer, and then incubated with primary antibodies followed by HRP-conjugated secondary antibodies (Table S1). Densitometric analyses of anti–acetylated-lysine Western blotting bands were performed by ImageJ software. Briefly, areas of Western blot bands larger than 28 kDa were framed as acetylated protein signals and then converted into gray values. After subtracting background values, the intensity profiles were determined and presented as a relative ratio. The acetylated protein signals larger than 28 kDa were divided into three sizes, namely: upper (> 75 kDa), middle (48–75 kDa), and lower (28–48 kDa) and then the linearity of signal intensities was validated by quantification of densitometric values of each area around 3-s exposure.

Measurement of hatching rate

Hatching rate was measured in reference to previous research (3). In brief, early L4 animals were bred on RNAi plates for 45 h, and then 6–8 gravid adults were transferred to new RNAi plates. These animals were removed 6 h thereafter, and then hatchlings and eggs were counted 24 h later.

Mitochondria/cytosol fractionation

In this fractionation, we referred to the protocol shown by Jonassen *et al.* (19). Large numbers of early embryos were collected by bleaching 35,000 gravid adults. The embryos were washed four times in M9 buffer, then resuspended in 2 ml of isolation buffer (IB) (210 mM mannitol, 70 mM sucrose, 0.1 mM EDTA, 5 mM Tris, pH 7.4, 1 mM PMSF). The samples were kept cold on ice throughout the fractionation procedure. The ani-

mals were homogenized with 15 up-and-down strokes with a Dounce homogenizer. The homogenates were centrifuged at 1000 × *g* for 10 min. The supernatants were saved, and 2 ml of IB were further added to the pellets. The pellets were resuspended and homogenized again with additional 15 strokes, and centrifuged at 1000 × *g* for 10 min. An aliquot of the combined supernatants was saved as total lysate (TL). The supernatants were centrifuged at 5000 × *g* for 10 min. The pellets were suspended with IB, and then centrifuged at 2000 × *g* for 10 min. The supernatants were saved, and another 1 ml of IB was added to the pellets. The pellets were resuspended and centrifuged at 2000 × *g* for 10 min. An aliquot of the combined supernatants was centrifuged at 14,000 × *g* for 10 min, and the mitochondrial pellet (MP) was obtained. The supernatants centrifuged at 5000 × *g* for 10 min were additionally centrifuged at 12,000 × *g* for 10 min. An aliquot of the resulting supernatant was saved as post-mitochondrial supernatant (PMS). Protein pellets of TL and PMS were collected by chloroform precipitation. SDS sample buffer was added to all pellets of TL, PMS, and MP.

Statistical analysis

Results were presented as mean ± S.E. Statistical significances were determined by two-tailed Student's *t* test using GraphPad Prism software. A p value < 0.05 was considered statistically significant.

Author contributions—K. Hada, K. Hirota, and A. F. conceptualization; K. Hada, K. Hirota, A. I., K. K., M. Miyata, S. A., M. Matsumoto, and R. O. data curation; K. Hada, K. Hirota, A. I., K. K., M. Miyata, S. A., and M. Matsumoto formal analysis; K. Hada and A. F. supervision; K. Hada, K. Hirota, A. I., K. K., M. Miyata, H. D., T. H., and A. F. funding acquisition; K. Hada, K. Hirota, K. K., M. Miyata, S. A., M. Matsumoto, R. O., M. A., and H. D. investigation; K. Hada, K. Hirota, K. K., M. Miyata, M. Matsumoto, R. O., H. D., and T. H. writing-original draft; K. Hada, K. Hirota, A. I., and A. F. project administration; K. Hada, K. Hirota, A. I., K. K., M. Miyata, H. D., T. H., and A. F. writing-review and editing; K. Hirota, A. I., M. Matsumoto, R. O., and M. A. methodology; R. O., M. A., and H. D. resources.

Acknowledgments—We thank Drs. Tsuyoshi Osawa (The University of Tokyo) and Teppei Shimamura (Nagoya University) for the helpful discussion. We also thank the members of Fukamizu Laboratory for technical advice. This work was partly performed in the Cooperative Research Project Program of the Medical Institute of Bioregulation, Kyushu University. Strains were provided by the Caenorhabditis Genetics Center and National BioResource Project.

References

1. Kane, M. T., and Buckley, N. J. (1977) The effects of inhibitors of energy metabolism on the growth of one-cell rabbit ova to blastocysts in vitro. *J. Reprod. Fertil.* **49,** 261–266 CrossRef Medline
2. Thomson, J. L. (1967) Effect of inhibitors of carbohydrate metabolism on the development of preimplantation mouse embryos. *Exp. Cell Res.* **46,** 252–262 CrossRef Medline
3. Rahman, M. M., Rosu, S., Joseph-Strauss, D., and Cohen-Fix, O. (2014) Down-regulation of tricarboxylic acid (TCA) cycle genes blocks progression through the first mitotic division in *Caenorhabditis elegans* embryos. *Proc. Natl. Acad. Sci. U.S.A.* **111,** 2602–2607 CrossRef Medline
4. Sönnichsen, B., Koski, L. B., Walsh, A., Marschall, P., Neumann, B., Brehm, M., Alleaume, A. M., Artelt, J., Bettencourt, P., Cassin, E., Hewitson, M., Holz, C., Khan, M., Lazik, S., Martin, C., *et al.* (2005) Full-genome RNAi profiling of early embryogenesis in *Caenorhabditis elegans*. *Nature* **434,** 462–469 CrossRef Medline
5. Pegg, A. E. (2008) Spermidine/spermine-N^1-acetyltransferase: A key metabolic regulator. *Am. J. Physiol. Endocrinol. Metab.* **294,** E995–E1010 CrossRef Medline
6. Verdin, E., and Ott, M. (2015) 50 years of protein acetylation: From gene regulation to epigenetics, metabolism and beyond. *Nat. Rev. Mol. Cell Biol.* **16,** 258–264 CrossRef Medline
7. Lundby, A., Lage, K., Weinert, B. T., Bekker-Jensen, D. B., Secher, A., Skovgaard, T., Kelstrup, C. D., Dmytriyev, A., Choudhary, C., Lundby, C., and Olsen, J. V. (2012) Proteomic analysis of lysine acetylation sites in rat tissues reveals organ specificity and subcellular patterns. *Cell Rep.* **2,** 419–431 CrossRef Medline
8. Anderson, K. A., and Hirschey, M. D. (2012) Mitochondrial protein acetylation regulates metabolism. *Essays Biochem.* **52,** 23–35 CrossRef Medline
9. Baeza, J., Smallegan, M. J., and Denu, J. M. (2016) Mechanisms and dynamics of protein acetylation in mitochondria. *Trends Biochem. Sci.* **41,** 231–244 CrossRef Medline
10. Hirschey, M. D., Shimazu, T., Jing, E., Grueter, C. A., Collins, A. M., Aouizerat, B., Stančáková, A., Goetzman, E., Lam, M. M., Schwer, B., Stevens, R. D., Muehlbauer, M. J., Kakar, S., Bass, N. M., Kuusisto, J., *et al.* (2011) SIRT3 deficiency and mitochondrial protein hyperacetylation accelerate the development of the metabolic syndrome. *Mol. Cell* **44,** 177–190 CrossRef Medline
11. McDonnell, E., Peterson, B. S., Bomze, H. M., and Hirschey, M. D. (2015) SIRT3 regulates progression and development of diseases of aging. *Trends Endocrinol. Metab.* **26,** 486–492 CrossRef Medline
12. Ghanta, S., Grossmann, R. E., and Brenner, C. (2013) Mitochondrial protein acetylation as a cell-intrinsic, evolutionary driver of fat storage: Chemical and metabolic logic of acetyl-lysine modifications. *CRC Crit. Rev. Biochem. Mol. Biol.* **48,** 561–574 CrossRef Medline
13. Tsuchiya, Y., Pham, U., Hu, W., Ohnuma, S., and Gout, I. (2014) Changes in acetyl CoA levels during the early embryonic development of *Xenopus laevis*. *PloS One* **9,** e97693 CrossRef Medline
14. Iacobazzi, V., and Infantino, V. (2014) Citrate—new functions for an old metabolite. *Biol. Chem.* **395,** 387–399 CrossRef Medline
15. Eisenberg, T., Knauer, H., Schauer, A., Büttner, S., Ruckenstuhl, C., Carmona-Gutierrez, D., Ring, J., Schroeder, S., Magnes, C., Antonacci, L., Fussi, H., Deszcz, L., Hartl, R., Schraml, E., Criollo, A., *et al.* (2009) Induction of autophagy by spermidine promotes longevity. *Nat. Cell Biol.* **11,** 1305–1314 CrossRef Medline
16. Morselli, E., Mariño, G., Bennetzen, M. V., Eisenberg, T., Megalou, E., Schroeder, S., Cabrera, S., Bénit, P., Rustin, P., Criollo, A., Kepp, O., Galluzzi, L., Shen, S., Malik, S. A., Maiuri, M. C., *et al.* (2011) Spermidine and resveratrol induce autophagy by distinct pathways converging on the acetylproteome. *J. Cell Biol.* **192,** 615–629 CrossRef Medline
17. Wirth, M., Karaca, S., Wenzel, D., Ho, L., Tishkoff, D., Lombard, D. B., Verdin, E., Urlaub, H., Jedrusik-Bode, M., and Fischle, W. (2013) Mitochondrial SIRT4-type proteins in *Caenorhabditis elegans* and mammals interact with pyruvate carboxylase and other acetylated biotin-dependent carboxylases. *Mitochondrion* **13,** 705–720 CrossRef Medline
18. Rustin, P., Bourgeron, T., Parfait, B., Chretien, D., Munnich, A., and Rötig, A. (1997) Inborn errors of the Krebs cycle: A group of unusual mitochondrial diseases in human. *Biochim. Biophys. Acta* **1361,** 185–197 CrossRef Medline
19. Jonassen, T., Marbois, B. N., Faull, K. F., Clarke, C. F., and Larsen, P. L. (2002) Development and fertility in *Caenorhabditis elegans* clk-1 mutants depend upon transport of dietary coenzyme Q8 to mitochondria. *J. Biol. Chem.* **277,** 45020–45027 CrossRef Medline
20. Park, M. H., and Igarashi, K. (2013) Polyamines and their metabolites as diagnostic markers of human diseases. *Biomol. Ther.* **21,** 1–9 CrossRef Medline
21. Lee, S. J., Murphy, C. T., and Kenyon, C. (2009) Glucose shortens the life span of *C. elegans* by down-regulating DAF-16/FOXO activity and aquaporin gene expression. *Cell Metab.* **10,** 379–391 CrossRef Medline

Tricarboxylic acid cycle activity suppresses acetylation of mitochondrial proteins during early embryonic development in *Caenorhabditis elegans*

Kazumasa Hada, Keiko Hirota, Ai Inanobe, Koichiro Kako, Mai Miyata, Sho Araoi, Masaki Matsumoto, Reiya Ohta, Mitsuhiro Arisawa, Hiroaki Daitoku, Toshikatsu Hanada and Akiyoshi Fukamizu

J. Biol. Chem. 2019, 294:3091-3099.
doi: 10.1074/jbc.RA118.004726 originally published online January 3, 2019